

Dark Matter Search with CALET

KENJI YOSHIDA¹ FOR THE CALET COLLABORATION.

¹ *Shibaura Institute of Technology, JAPAN*

yoshida@shibaura-it.ac.jp

Abstract: The CALorimetric Electron Telescope, CALET, is a high-energy astroparticle physics mission to be installed on the International Space Station in 2014. Its main instrument, CALET-CAL, will take a whole sky survey of the electrons and gamma-rays in the energy range from 10 GeV to more than 10 TeV with an energy resolution of 1~3 %. Since electron spectral and gamma-ray line signatures are expected in the sub-TeV to TeV region, due to annihilation or decay of dark matter particles, the CALET-CAL is sensitive to both these signatures. In this paper, we present the expected performance of CALET-CAL for a dark matter search.

Keywords: Dark matter, electron, gamma ray, ISS

1 Introduction

The existence of dark matter in the Universe is identified by numerous observations such as Cosmic Microwave Background (CMB) measurements, observations of cluster of galaxies, and rotation curves of spiral galaxies. However, till now, nobody knows what the dark matter is made of. The nature and origin of dark matter is one of the most important unresolved problem in astrophysics. The most plausible class of candidates for dark matter is some weakly interacting massive particles (WIMPs) which could have been thermally produced in the very early universe. Since these WIMP dark matters are expected to annihilate and/or decay into gamma rays, electrons, and positrons, WIMP dark matter may be identified by the observations of these products. The recent observations of the positron excess with PAMELA [1] and AMS-02 [2], and a tentative gamma-ray line feature with Fermi-LAT [3, e.g.] warm up the discussion, and many theoretical dark matter models are proposed in order to explain the observed data.

The CALET-CAL, the main instrument of CALET on the ISS, has a capability to take a whole sky survey of the electrons + positrons and gamma rays in the energy range from 10 GeV to more than 10 TeV with an excellent energy resolution of 1~3 % [4]. The CALET-CAL capability enables us to carry out a dark matter search.

2 Electron observations

2.1 Positron fraction

A precise measurement by AMS-02 on the International Space Station of the positron fraction in the energy range from 0.5 to 350 GeV shows that the positron fraction is steadily increasing from 10 to ~200 GeV [2]. The AMS-02 result is consistent with the positron fraction observed by PAMELA [1]. These results cannot be understood by standard models describing the secondary production of cosmic rays. The observations require the existence of new physical phenomena, from a particle physics or an astrophysical origin.

In order to explain the observed positron fraction, Aguilar et al. (2013) [2] adopted a minimal model, as an example, in which the e^+ and e^- fluxes, Φ_{e^+} and Φ_{e^-} , respectively,

are parameterized as the sum of individual power-law spectra and the common single power-law spectrum with an exponential cutoff. We refer to their minimal model as the empirical model (A).

$$\Phi_{e^-} = C_{e^-} E^{-\gamma_{e^-}} + C_s E^{-\gamma_s} e^{-E/E_s} \quad (1)$$

$$\Phi_{e^+} = C_{e^+} E^{-\gamma_{e^+}} + C_s E^{-\gamma_s} e^{-E/E_s} \quad (2)$$

Here, the coefficient C_{e^-} , C_{e^+} and C_s are normalization factors for the power-law spectra, γ_{e^-} , γ_{e^+} and γ_s are the corresponding power-law indices, and E_s is an exponential cutoff energy for the common source spectrum, which represents the spectrum from physical phenomena such as dark matter or a nearby pulsar. The parameters are same as Aguilar et al. (2013) [2], and the exponential cutoff energy E_s is parameterized as 760 GeV. The other parameters are as follows: $\gamma_{e^-} - \gamma_{e^+} = -0.63$, $\gamma_{e^-} - \gamma_s = 0.66$, $C_{e^+}/C_{e^-} = 0.091$, and $C_s/C_{e^-} = 0.0078$.

The higher cutoff energy of $E_s = 1.4$ TeV can also represent the AMS-02 positron fraction, as shown in Fig. 1. We refer to the higher exponential cutoff model as the empirical model (B). The parameters are as follows: $\gamma_{e^-} - \gamma_{e^+} = -0.69$, $\gamma_{e^-} - \gamma_s = 0.61$, $C_{e^+}/C_{e^-} = 0.099$, $C_s/C_{e^-} = 0.0093$, and $E_s = 1.4$ TeV.

As another empirical model, we adopted the empirical model (C) with a super exponential cutoff in the following.

$$\Phi_{e^-} = C_{e^-} E^{-\gamma_{e^-}} + C_s E^{-\gamma_s} e^{-(E/E_s)^\alpha} \quad (3)$$

$$\Phi_{e^+} = C_{e^+} E^{-\gamma_{e^+}} + C_s E^{-\gamma_s} e^{-(E/E_s)^\alpha} \quad (4)$$

The parameter $\alpha(> 1)$ describes a steeper cutoff than an exponential cutoff. The parameters are as follows: $\gamma_{e^-} - \gamma_{e^+} = -0.67$, $\gamma_{e^-} - \gamma_s = 0.58$, $C_{e^+}/C_{e^-} = 0.090$, $C_s/C_{e^-} = 0.0099$, $E_s = 1.4$ TeV, and $\alpha = 7.0$. As shown in Fig. 1, the empirical model (C) also well represents the positron fraction measured by AMS-02.

The secondary positrons are mostly decay products of charged pions produced mainly by interactions of cosmic-ray protons and nuclei with interstellar gas. As positrons are produced by the process $\pi^\pm \rightarrow \mu^\pm \rightarrow e^\pm$, the spectral index of secondary positrons is the same as the index $\simeq 2.7$ of the parent cosmic-ray protons and nuclei. This index is larger than the index ~ 2.1 of primary electrons at the primary

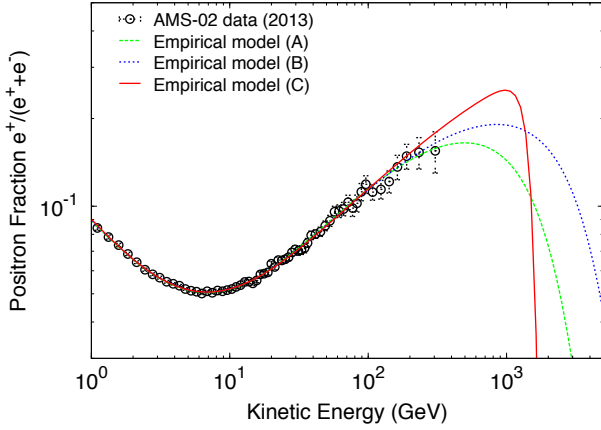


Fig. 1: Positron fraction measured by AMS-02 [2] compared with the empirical models. The empirical model (A) with $E_s = 760$ GeV is the same as the minimal model described in Aguilar et al. (2013) [2]. The empirical model (B) with $E_s = 1.4$ TeV has the same formula, but the higher cutoff energy of 1.4 TeV. The empirical model (C) is a super exponential cutoff model with the cutoff energy of 1.4 TeV. See text for details.

source. Hence, the index difference of $\gamma_{e^-} - \gamma_{e^+}$ is estimated to be ~ -0.6 , which is consistent with that of the empirical models.

While propagating through the Galaxy, the electrons and positrons lose their energy E , mainly via the synchrotron and inverse Compton processes. The energy-loss rate, dE/dt , is given by

$$\frac{dE}{dt} = -bE^2, \quad b \simeq (1-2) \times 10^{-16} \text{ GeV}^{-1} \text{ s}^{-1}. \quad (5)$$

Therefore, the propagation of the mono-energetic electrons and positrons through the Galaxy modify their energy spectra to be a power-law with an index of -2.0 and a cutoff energy characteristic of the dark matter mass. As the index difference of $\gamma_{e^-} - \gamma_s$ is estimated to be ~ 1.0 for the mono-energetic positrons, the empirical models indicate steeper power-law indices than that of the mono-energetic positrons.

2.2 Electron + positron spectrum

We also applied the empirical models (A), (B), and (C) to the electron + positron spectra. Figure 2 presents the observed electron + positron spectra [5, and references therein], compared with the empirical model (A), (B) and (C). The electron power-law index of γ_{e^-} is taken as 3.20 in common with the three models. The electron normalization factors of C_{e^-} are $2.74 \times 10^2 \text{ m}^{-2} \text{ s}^{-1} \text{ sr}^{-1} \text{ GeV}^{-1}$ for model (A) and $2.71 \times 10^2 \text{ m}^{-2} \text{ s}^{-1} \text{ sr}^{-1} \text{ GeV}^{-1}$ for model (B), respectively. As shown in Fig. 2, the empirical model (A) with the cutoff energy of 760 GeV does not represent very well the electron + positron spectra observed with Fermi-LAT and PAMELA [6, 7]. The observed electron + positron spectra require much higher cutoff energies. Figure 2 shows that the empirical model (B) with the higher cutoff energy of 1.4 TeV well represents the observed spectra. Figure 2 also presents the empirical model (C). The electron normalization factors of C_{e^-} are $2.64 \times 10^2 \text{ m}^{-2} \text{ s}^{-1} \text{ sr}^{-1} \text{ GeV}^{-1}$ for

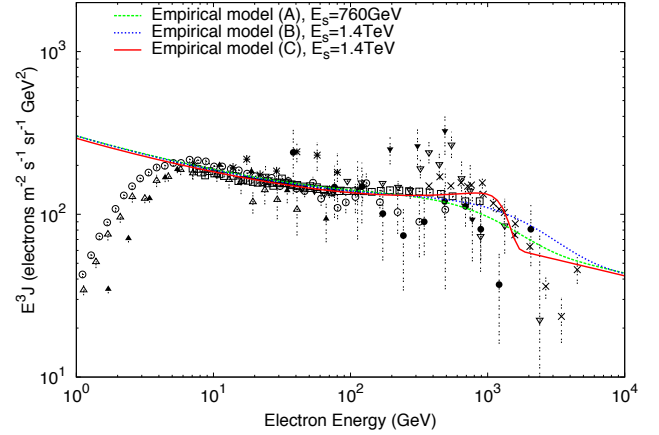


Fig. 2: The empirical model (A), (B), and (C), compared with the observed electron + positron spectra [5, and references therein].

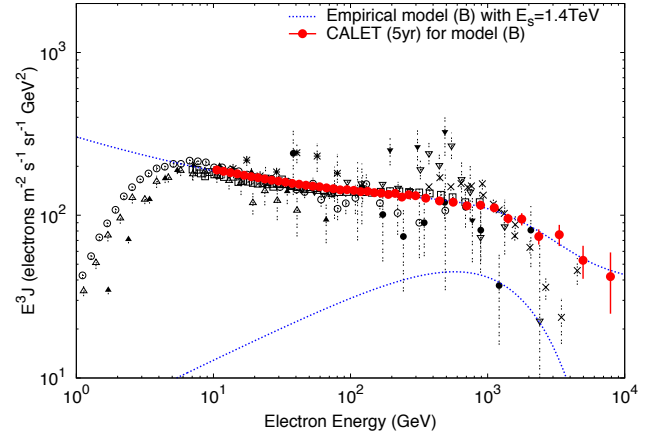


Fig. 3: The expected electron + positron spectrum for CALET-CAL 5 year observations with the model (B).

model (C). The empirical model (C) also well represents the electron + positron spectra observed with Fermi-LAT and PAMELA [6, 7].

The simulated electron + positron spectrum with the empirical model (B) and (C) for the CALET-CAL 5 year observations are presented in Fig. 3 and Fig. 4, respectively. As shown in Fig. 3 and Fig. 4, CALET-CAL has a capability to distinguish between the exponential cutoff and the steeper cutoff of the contribution of a single common source component.

2.3 Anisotropy

In addition to scenarios of annihilating or decaying dark matter, nearby pulsars such as B0355+54 (1.1 kpc, 5.6×10^5 yr) [8] and B0656+14 (0.29 kpc, 1.1×10^5 yr) [9] are also indicated as the candidates to explain the excess in the positron fraction observed with PAMELA and AMS-02. Since the nearby pulsars are expected to show the anisotropy of the electrons + positrons, the anisotropy observations will bring us important information to identify the possible sources.

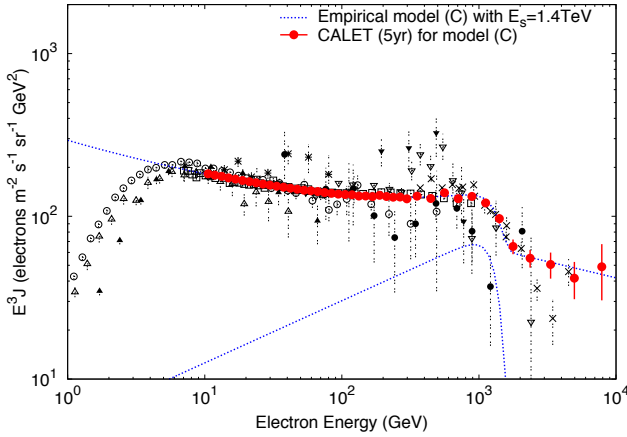


Fig. 4: The expected electron + positron spectrum for CALET-CAL 5 year observations with the model (C).

For an individual source located at distance r_i and of age t_i , the anisotropy parameter δ_i is given by

$$\delta_i = \frac{I_{max} - I_{min}}{I_{max} + I_{min}} = \frac{3r_i}{2ct_i}, \quad (6)$$

where I_{max} and I_{min} are the maximum and minimum intensity in all directions.

For CALET-CAL 5 year observations above 10 GeV, we calculated the significance levels for anisotropies of electrons + positrons between distance and age of nearby pulsars. In this calculation, we assumed that the electrons and positrons are continuously released from nearby pulsars. If B0355+54 at the distance of 1.1 kpc and the age of 5.6×10^5 yr or B0656+14 at the distance of 0.29 kpc and the age of 1.1×10^5 yr is the source of the positron excess, CALET-CAL will detect the anisotropy with a statistical significance above 8σ .

3 Gamma-ray observations

Monochromatic gamma-ray signals from WIMP dark matter would provide a distinctive signature of dark matter if detected. Since gamma-ray line signatures are expected in the sub-TeV to TeV region, due to annihilation or decay of dark matter particles, the CALET-CAL with the excellent energy resolution of $1 \sim 3\%$ above 100 GeV is a suitable instrument to detect these signatures. The expected performance of CALET-CAL as a gamma-ray detector will be presented in the accompanying papers [10, 11].

The gamma-ray flux from WIMP dark matter annihilations in the dark matter profile is given by

$$\Phi_\gamma = \frac{N_\gamma \sigma v}{m_\chi^2} J, \quad (7)$$

where N_γ is the number of gamma rays created per annihilations, σv is the annihilation cross section times the relative velocity of the annihilating particles, m_χ is the mass of WIMPs, and J is the astronomy dependent part of

$$J = \frac{1}{4\pi} \int \int_{line\ of\ sight} \rho^2(\ell) d\ell d\Omega, \quad (8)$$

where $\rho(\ell)$ is the halo mass density of WIMPs at distance ℓ along the line of sight.

The values of J depend on the dark matter density distribution in the Galactic halo. Various dark matter distributions are calculated by different N -body simulations such as Navarro, Frenk and White (NFW, 1996) [12], Moore *et al.* (1999) [13] and isothermal halo profile. Normalized to the value of J for the isothermal halo profile, the value of J is $\sim 10^2$ for NFW halo profile and $\sim 10^4$ for Moore halo profile. N -body simulations also indicate that the dark matter distributions have clumpy structures in the Galactic halo. Clumpy distributions of WIMP dark matter still increase the gamma-ray flux in proportion to the square of dark matter density. This effect increases the gamma-ray flux with an amplitude of $10^2 - 10^3$, which is often described as a boost factor.

As for the annihilation cross-section, the present gamma-ray observations indicate that the annihilation cross-section is less than $\langle \sigma v \rangle \sim 10^{-24} \text{ cm}^3 \text{ s}^{-1}$ for $m_\chi = 1 \text{ TeV}$ [14]. By now, HESS observations of the Galactic center provide the strongest limits on dark matter annihilation with 700 GeV, down to annihilation cross-sections of $4 \times 10^{-25} \text{ cm}^3 \text{ s}^{-1}$ [14]. These limits are derived for assumptions on the dark matter profile, NFW profiles in most cases. The positron excess observed with AMS-02 corresponds to the annihilation cross-section of $\langle \sigma v \rangle_{e^+e^-} \sim 10^{-24} \text{ cm}^3 \text{ s}^{-1}$ [15, e.g.].

As a minimal model, for example, we adopted the dark matter mass of 1.4 TeV, annihilation into $\gamma + \gamma$, the annihilation cross-section of $\langle \sigma v \rangle_{\gamma\gamma} = 1 \times 10^{-25} \text{ cm}^3 \text{ s}^{-1}$, and the NFW dark matter halo profile.

Figure 5 presents the simulated spectrum of 1.4 TeV gamma-ray line from dark matter annihilations toward the Galactic center ($300^\circ < \ell < 60^\circ, |b| < 10^\circ$) including the Galactic diffuse background for CALET-CAL 5 year observations. The annihilation cross-section is taken as $\langle \sigma v \rangle_{\gamma\gamma} = 1 \times 10^{-25} \text{ cm}^3 \text{ s}^{-1}$ with a NFW halo profile. As shown in Fig. 5, CALET-CAL has the capability to detect a monochromatic gamma-ray signal from dark matter in the TeV region. The CALET-CAL sensitivity of gamma-ray lines above 10 GeV is $4 \times 10^{-9} \text{ cm}^{-2} \text{ s}^{-1}$, corresponding to 10 photons, for 1 year observations.

4 Summary

The nature and origin of dark matter has remained a major physics mystery, since Zwicky [16] first identified the problem almost 80 years ago. The CALET-CAL has the ability to measure the spectral shape, the characteristic energy, the presence or absence of the anisotropy of the electrons + positrons, and the gamma-ray line signature from WIMP dark matter in the sub-TeV to TeV region. CALET will be installed on the JEM-EF on the ISS in 2014, opening a new window on a dark matter search.

References

- [1] O. Adriani et al. (Pamela Collaboration), Nature 458, 607-609, 2009
- [2] M. Aguilar et al. (AMS Collaboration), Phys. Rev. Lett. 110, 141102, 2013
- [3] C. Weniger, JCAP 08, 007, 2012
- [4] S. Torii et al., Proc. of 33rd ICRC (Rio de Janeiro), 2013

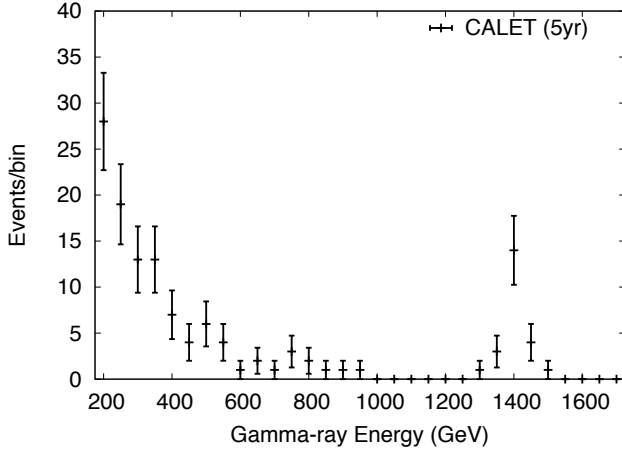


Fig. 5: Simulated 1.4 TeV gamma-ray line from dark matter toward the Galactic center including the Galactic diffuse background for CALET-CAL 5 year observations. The annihilation cross-section is taken as $\langle\sigma v\rangle_{\gamma\gamma} = 1 \times 10^{-25} \text{ cm}^3\text{s}^{-1}$ with a NFW halo profile.

- [5] T. Kobayashi et al., *Astrophys. J.* 760, 146-158, 2012
- [6] M. Ackermann et al. (Fermi-LAT Collaboration), *Phys. Rev. D* 82, 092004, 2010
- [7] O. Adriani et al. (Pamela Collaboration), *Phys. Rev. Lett.* 106, 201101, 2011
- [8] S. Profumo, arXiv:0812.4457v1 [astro-ph], 2008
- [9] D. Hooper et al., *JCAP*01, 025, 2009
- [10] M. Mori et al., *Proc. of 33rd ICRC (Rio de Janeiro)*, 2013
- [11] A. Moiseev et al., *Proc. of 33rd ICRC (Rio de Janeiro)*, 2013
- [12] J. F. Navarro, C. S. Frenk and S. D. M. White, *Astrophys. J.* 462, 563, 1996
- [13] B. Moore et al., *Mon. Not. R. Astron. Soc.* 310, 1147, 1999
- [14] T. Bringmann and C. Weniger, *Dark Universe* 1, 194-217, 2012
- [15] J. Kopp, arXiv:1304.1184v1 [hep-ph], 2013
- [16] F. Zwicky, *Helv. Phys. Acta* 6, 110, 1993